ScienSage

Journal of Advanced Scientific Research

Available online through http://www.sciensage.info

ISSN
0976-9595
Research Article

PHOTOLUMINESCENCE INVESTIGATIONS OF TRANSITION METAL (Ni, Co) DOPED ZnS NANOCRYSTALS

Prashant Kumar Singh*[1, 2], Manvendra Kumar[3], Anil Kumar[4], Sindhu Singh[4], Shanthy Sundaram[5], Avinash C Pandey[1, 6]

[1]*Nanotechnology Application Centre, Faculty of Science, University of Allahabad, Prayagraj, India*

[2]*Department of Applied Science and Humanities, I.E.T., Dr. Rammanohar Lohia Avadh University, Ayodhya, India*

[3]*Department of Physics, Institute of Science, Shri VaishnavVidyapeeth Viswavidyalaya, Indore, India*

[4]*Department of Physics and Electronics, Dr Rammanohar Lohia Avadh University, Ayodhya, India*

[5]*Centre of Biotechnology, Nehru Science Complex, University of Allahabad, Prayagraj, India*

[6]*Inter University Accelerator Centre, Aruna Asaf Ali Road, New Delhi, India*

**Corresponding author: prashant2singh@gmail.com*

ABSTRACT

In the present investigation, Nickle and Cobalt (Transition metals) doped ZnS Nanocrystals were synthesized by wet chemical route using methanol water binary mixture as a solvent. 1-20% doped percent of dopant were used. The synthesized samples were characterized by X-ray diffraction (XRD), transmission electron microscopy (TEM), selected area electron diffraction (SAED), and photoluminescence (PL) spectroscopy for structural and optical investigations. Phase and structural analysis confirmed the formation of cubic ZnS having nearly spherical shaped nanoparticles having size ~3 nm. PL spectra showed broad and asymmetric band centered nearly at 435 nm. The intensity of PL peaks showed gradual quenching with increasing dope percentage which makes it unsuitable for biological imaging applications.

Keywords: ZnS, Transition metals doped, Photoluminescence (PL), Quenching.

1. INTRODUCTION

ZnS has been extensively investigated wide band-gap (~ 3.6 eV) semiconductor material because of their size dependent optical properties and their wide range of applications in sensors, displays, electronic devices, laser devices and nonlinear optical devices, etc. [1-5]. ZnS is among the oldest and probably the most important materials used as phosphor host [6]. In the past decade, many research articles [7-15] have been reported on the synthesis of nanometer scale semiconductor crystals (quantum dots, nano-wires, nano-rods, etc.) because of their properties, due to quantum confinement effect [16-18], dramatic change and in most cases, improvement as compared with their bulk counterparts [19-20]. In the early 1980s, considerable work on properties of colloidal prepared ZnS nano-clusters has been reported [16, 21]. The main contributions of these studies have demonstrated the size-dependent effect of the basic physical and their optical properties of the un-doped nano-particles. Doping plays a critical role for semiconductors, which would otherwise be electrically insulating. For this reason, researchers have started to explore how dopants can determine the size and shape-specific optical and electronic properties of semiconductor nano-crystals (NCs) [19]. The use of intentional impurities or dopants to control the properties of materials lies at the heart of many technologies. By doping ZnS with different metals [21-24], a variety of luminescent properties excited by UV, X-rays, cathode rays and electroluminescence have been observed. The doping of 3d transition-metal (TM) impurities in semiconductors form deep levels within the band gaps of the host materials. They are technologically important as luminescence centers and charge compensations as well as unwanted traps. Since Bhargava and his co-workers reported the novel properties in nano-sized ZnS doped with Mn^{2+} ions [21], many studies have been published on Ti, V, Cr, Mn, Fe, Co, Ni, Cu and rare-earth metal ions activated II-VI, III-V and I-III-VI nanometer scale semiconductor materials [17, 25-31]. Novel luminescence characteristics such as stable and visible-light emissions with different colors were

observed from doped ZnS nano-crystals at room temperature [17, 27, 32-34].

In 1998, first report of the application of luminescent nano-crystals as biological labels appeared in two breakthrough papers [35-36]. Both groups simultaneously demonstrated that highly luminescent semiconductor nano-crystals could be made water-soluble and biocompatible by their suitable surface modification and bioconjugation. They also showed the high potential of nano-crystals as highly sensitive fluorescent biomarkers and (bio) chemical probes. Other key advances enabling the emerging practical applications of nano-crystals in biochemistry and medicine included the synthesis of high-quality colloidal nano-crystals in large quantities [37] or recent advances on surface chemistry of nano-crystals by conjugation with appropriate functional molecules [38]. The surface modification of nano-crystals can enhance their luminescent quantum yields [38], improve stability of the nano-crystals as well as prevent them from aggregating [39], and make nano-crystals available for interactions with target analytes [40], all of crucial interest for chemical sensor or biosensor applications. In the past years, the progress in synthesis and optimization of nano-crystals for biological environments has opened the doors to an expanding variety of biological applications, such as serving as specific markers for cellular structures and molecules, tracing cell lineage, monitoring physiological events in live cells, measuring cell motility and tracking cells *in vivo* etc.

In this paper, we have demonstrated synthesis of Nickle and Cobalt doped ZnS nano-crystals by simple wet chemical route using ethanol water mixture (75:25) as solvent. The synthesized nano-crystals were characterized by X-ray diffraction (XRD), Transmission electron microscopy (TEM) and photoluminescence (PL) spectroscopy. The effect of dopant on optical properties of ZnS nano-crystals has been investigated in view of suitable candidate for biomedical investigation.

2. EXPERIMENTAL

2.1. Material

Zinc acetate dehydrated [$Zn(CH_3COO)_2.2H_2O$], Manganese(II) acetate tetra hydrate [$(CH_3COO)_2$ Mn $4H_2O$],Nickel(II) chloride hexahydrate ($NiCl_2 \cdot 6H_2O$), Chromium(II) chloride ($CrCl_2$), Sodium sulfide (Na_2S) flakes and methanol were purchased from Merck India Limited, Mumbai, India. All the chemicals were of analytical grade and were used as purchased without further purification.

2.2. Synthesis of nano-crystals (NCs)

The nano-crystals were synthesized by simple wet chemical route using co-precipitation reaction, which has been proven an effective colloidal chemical method for preparing compound nano-particles [41-43]. First, the NCs were synthesized in varying solvent composition from pure double distilled water to pure methanol. By comparing the properties of materials obtained from these different solvent mixtures, we have optimized the 75:25 of methanol and water binary mixture as solvent which was the best choice for producing efficient luminescent nano-phosphors in terms of process simplicity, effectiveness in doping and higher yield.

For preparation of TM doped nano-crystals, water/methanol binary solution (with 75% methanol in volume ratio) of zinc acetate, nickel (II) acetate and sodium sulfide were used as a stock solution. In a typical reaction, 50 ml of 0.5 M Zinc acetate solution was added with required volume of 0.01 M Nickel (II) acetate solution to obtain desired Ni^{2+} concentration (1-20%) in the medium. The solution was stirred well for 30 min on a magnetic stirrer at room temperature. 50 ml of 0.5 M Sodium sulfide solution was added dropwise under vigorous stirring. This mixing was done with flow rate of 1 ml/min at room temperature. White turbidity appeared at the junction of the mixture shows the formation of nano-crystals. The precipitate was collected by centrifugation at 3000 rpm and washed three times with the methanol/water binary solution and followed by methanol in order to remove unnecessary impurities. The obtained white product was vacuum dried for overnight at 50°C to get white powders of $ZnS:Ni^{2+}$. Similar processes was followed to prepare the Co doped ZnS nano-crystals.

2.3. Characterizations

The synthesized TM doped ZnS Nanocrystals were characterized by X-ray diffraction (XRD), Transmission electron microscopy (TEM), UV-Vis Spectroscopy and Photoluminescence spectroscopy (PL) for detailed structural and optical investigations. XRD was performed on Rigaku D/max-2200 PC diffractometer (with CuK_{α_1} radiation with wavelength of 1.54 Å) operated at 40 kV/20 mA, in the wide angle region from 10° to 70° on 2θ scale and the phase identification was carried out with the help of standard JCPDS database. The crystallite size was calculated from the full width at half maximum of the major XRD peak using Scherrer's formula [44]. The size and morphology of prepared

nano-crystals were measured using a transmission electron microscope (model Technai $30G^2$ S-Twin electron microscope) operated at 300 kV accelerating voltage. Sample for TEM was prepared by dissolving the as-synthesized powder sample in ethanol and then placing a drop of this dilute ethanolic solution on the surface of carbon coated 300 mesh copper grid and the grid was dried in air. Optical absorption spectra were recorded on Perkin Elmer Lambda 35 UV visible spectrophotometer using halogen and deuterium lamps as sources for visible and UV radiations, respectively, by dispersing TM doped nano-crystals in double distilled water and using double distilled water as a reference. Photoluminescence (PL) studies were performed for λ_{ex} = 325 nm on a Perkin Elmer LS 55 luminescence spectrophotometer using a Xenon discharge lamp, equivalent to 20 kW for 8 microsecond duration as the excitation source at room temperature. All the measurements were carried out at room temperature.

3. RESULTS AND DISCUSSIONS

3.1. XRD-Analysis

Fig.1 shows the wide-angle XRD pattern of as prepared ZnS:Co^{2+}(a), and ZnS:Ni^{2+}(b) nano-crystals with varying percentage of doping. The doped mole percent ratios of TM^{2+} were 1.0, 5.0, 10.0, 15.0 and 20.0, respectively. XRD spectra show broad peaks at positions of 28.68°, 47.83° and 56.49° corresponding to (111), (220) and (311) reflections, which are in good agreement with the standard JCPDS file for cubic ZnS (JCPDS 77-2100) for all the samples. There is no significant change in the XRD pattern as we increase the percentage of the Transition metals doping in the nano-crystals, which clearly indicates that the cubic structure of ZnS is not tailored by the addition of TM into the ZnS crystal system at least up to the detection level of XRD. The XRD peaks tend to broaden and their widths become larger as the particles become smaller due to the finite size of these crystallites. From XRD analysis, no characteristic peaks of impurity phases have been observed for any of the prepared doped samples. All the available reflections of the present XRD phases have been fitted with Gaussian distribution. The particle size, *d*, of nano-crystals were estimated by Debye-Scherrer's equation given below

$$d = \frac{0.9\lambda}{B\cos\theta}$$

where, *d* is the particle size, λ is the wavelength of radiation used, θ is the Bragg angle and *B* is the full width at half maxima (FWHM) on 2θ scale. The average crystallite size was estimated for the most prominent X-ray diffraction, corresponding to (111) peak at 28.57°, and was found ~2-4 nm. The almost same crystallite size, stable cubic zinc-blend structure, and absence of impurity phases with increasing concentration of TM doping for all the samples could be attributed to the similarity of size of Zn and doped ions. This is mainly because of the same nucleation and subsequent growth rate with increasing TM doping percentage. Ionic radius of Co^{2+} is 0.83 Å, for Ni^{2+} is 0.80Å it is almost same to that of Zn^{2+} i.e. 0.74 Å(43).

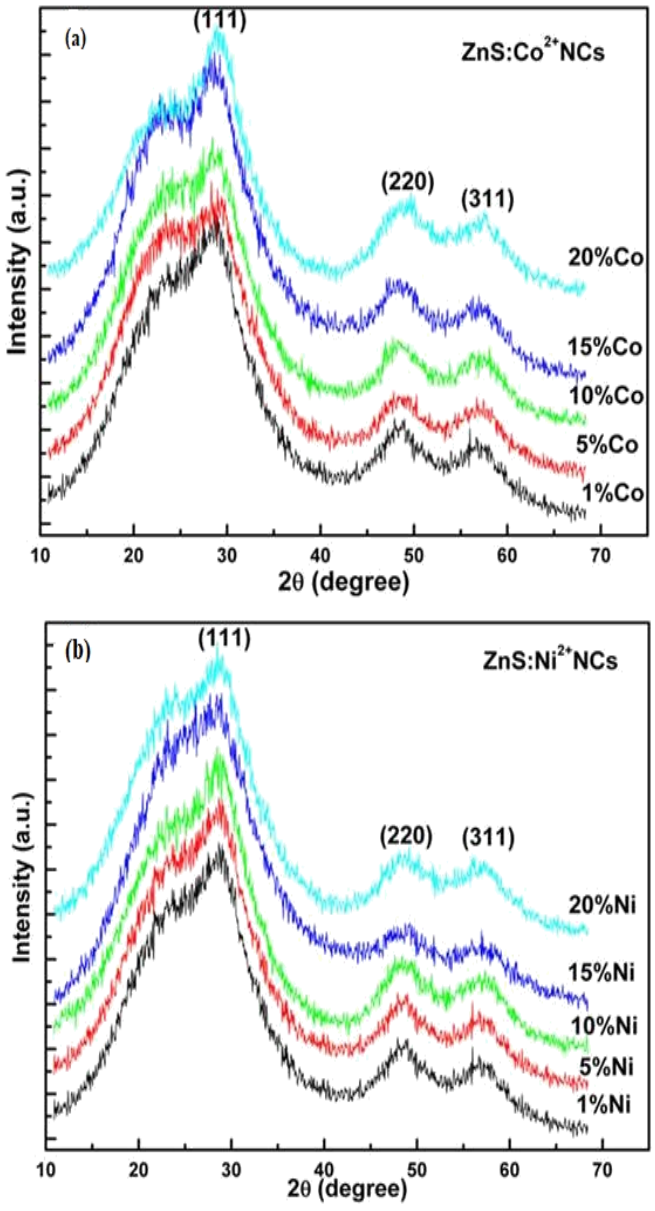

Fig. 1: X-Ray Diffraction Pattern of TM doped ZnS Nano-crystals (a) ZnS:Co^{2+} (b) ZnS:Ni^{2+}.

3.2. TEM Analysis

Fig.2 shows the representative TEM images of the as-prepared TM doped ZnS NCs for 10% doping. Fig 2(a) and 2 (b) are the TEM and HRTEM of ZNS:Co^{2+} NCs, respectively. Similarly, 2(c), 2(d) are TEM and HRTEM ZnS:Ni^{2+}, respectively. It can be seen that the resultant ZnS NCs are uniform spherical-shaped particles, 3 nm in diameter, and with a very narrow size distribution (the particle size distribution histogram is shown in the inset of Fig. 2 of respective HRTEM for each of the TM doped ZnS NCs. The difference of this value with the particle size calculated from Scherrer's formula may be due to the particle size and shape distribution involved and the average value obtained from the calculation. The HRTEM image of the TM doped ZnS NCs demonstrates the high crystallinity of the ZnS NCs, and the distances (0.258 nm) between the adjacent lattice fringes are the interplanar distances of ZnS (111) plane for every case. The selected area electron diffraction (SAED) pattern (inset of the respective TEM Figure) indicates that the TM doped ZnS NCs possess high crystallinity and a cubic structure, in which the three diffraction rings are perfectly indexed to the same positions as those from ZnS.

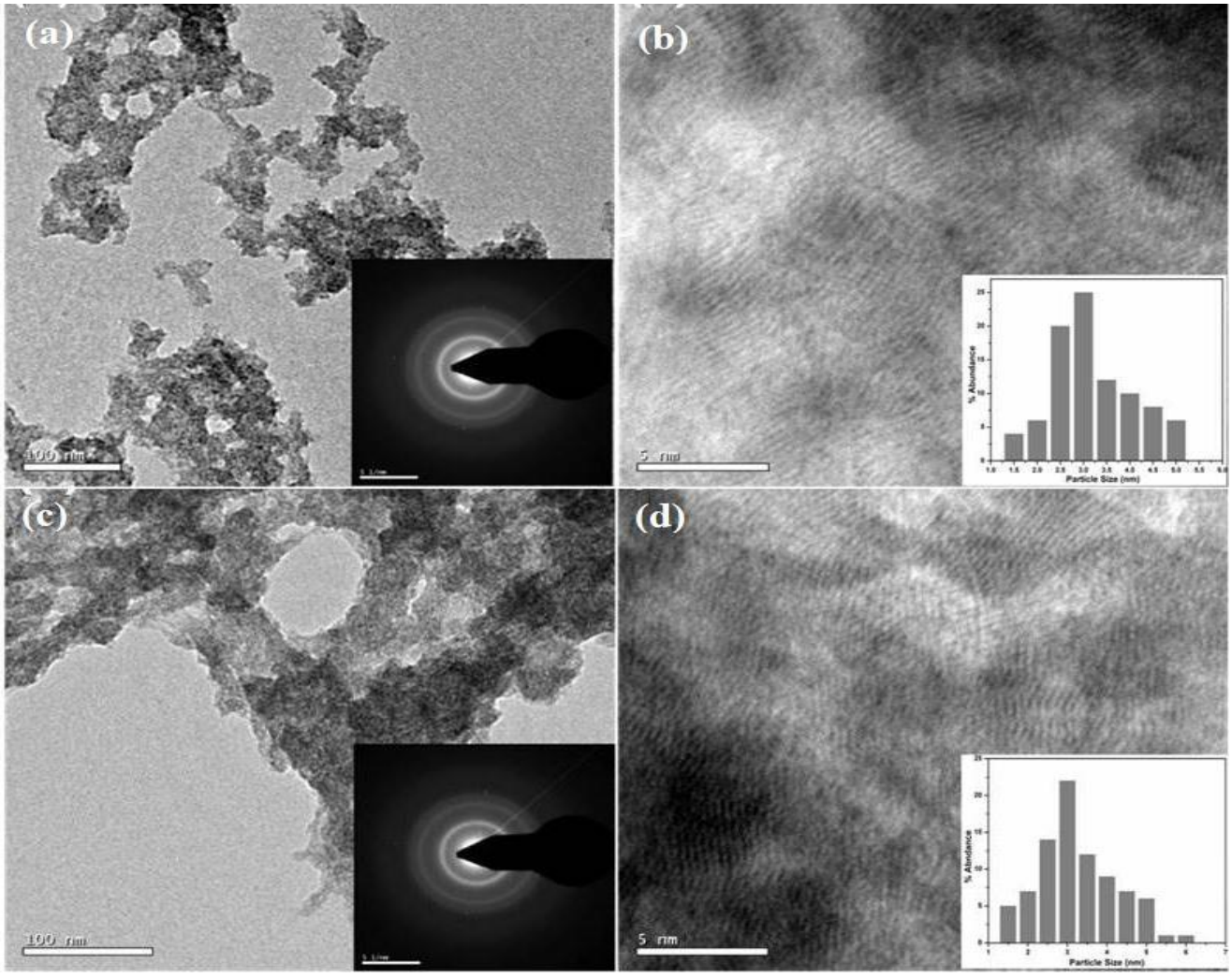

Fig. 2: Representative TEM Micrograph of TM Doped Samples (a) ZnS:Co^{2+}(b) HRTEM of ZnS:Co^{2+}(c) ZnS:Ni^{2+}(d) HRTEM of ZnS:Ni^{2+}, insets show the corresponding SEAD pattern and Particle Size Distribution.

3.3. Photoluminescence of the Nano-crystals

Fig.3 shows the room temperature PL spectra of Ni^{2+} and Co^{2+} doped ZnS sample. Fig. 3a and 3b show the PL spectra of Co^{2+} doped ZnS and Ni^{2+} doped ZnS nano-crystals respectively. The spectra are broad and asymmetric, so it should consist of more than one

component. Gaussian curve fitting was employed to de-convolute the PL curves of Co^{2+} doped and Ni^{2+} doped ZnS (Fig.4 and Fig.5, respectively).

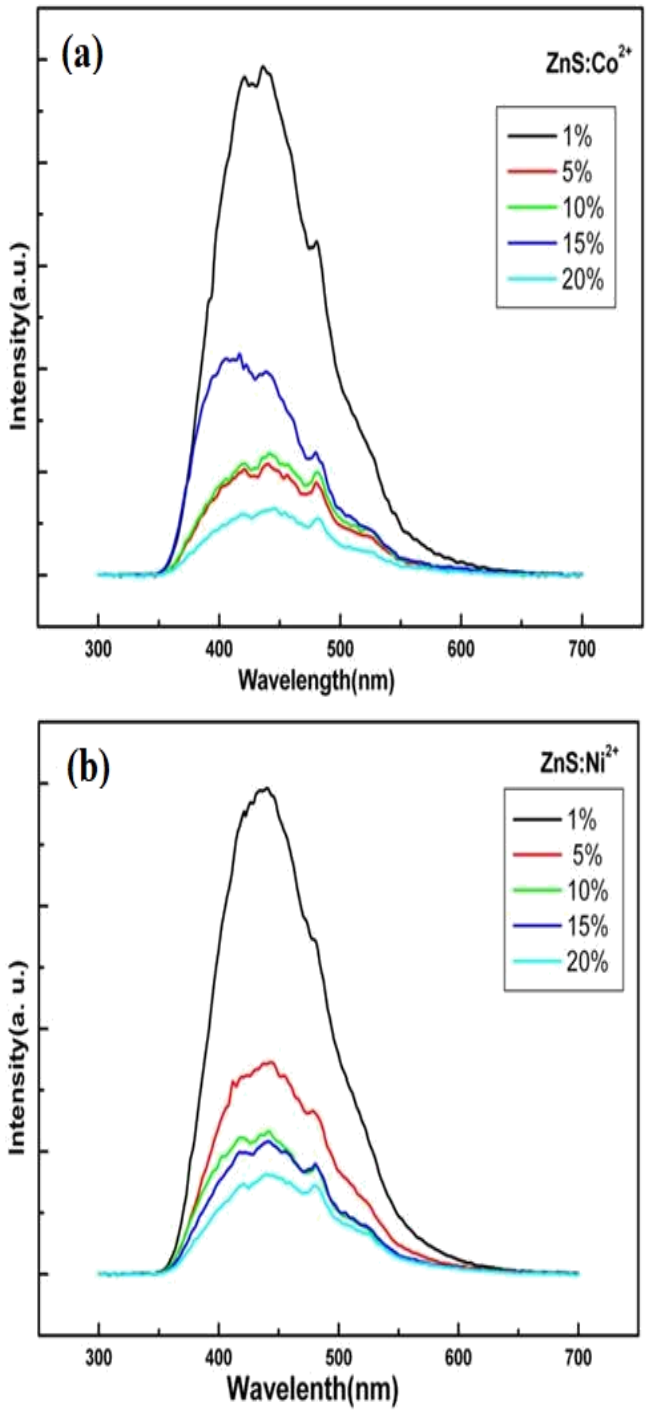

Fig. 3: Photoluminescence Spectra of TM Doped ZnS NCs (a) ZnS:Co^{2+}(b) ZnS:Ni^{2+}.

The PL spectrum of ZnS:Co^{2+} and ZnS:Ni^{2+} NCs were de-convoluted into three weak peaks, which are centered at 413, 451 and 496 nm, respectively. The fitting results are listed in Table 1 and Table 2 for Co and Ni doped NCs, respectively. The PL peak at 413 nm is known to be due to the recombination between the sulfur vacancy-related donor and valence band [46]. The emission peak at about 451 nm is attributed to the trap state emission of ZnS, related with native zinc vacancy. In ZnS nano-particles [11, 47] and ZnMnS nano-belts [48], the similar luminescence around this wavelength (450 nm) was also reported. Peak at 520 nm is due to the recombination between the donor vacancies of sulfur and Co and Ni related accepter [46, 49]. Form the PL spectra, it is clear that with increasing the concentration of both the dopants i.e. by doping cobalt or nickel, a dramatic quenching of photo--luminescence intensity was observed. The possible reason for the quenching of luminescence by doping of cobalt and nickel may be that, the nickel and cobalt are doped substitutionally in bulk ZnS [50, 51]. They act as electron trapping centers which results into non-radiative recombination. This means that photo-excited electrons are preferentially transferred to nickel and cobalt metal ion induced trapping centers compared to anion vacancy defect centers. Similar type of quenching of PL peak ~425 nm in ZnS colloidal particles by Cd^{2+} ions was investigated by Weller *et al*. [52].

Table 1: Photoluminescence Peak Position in the ZnS:Co^{2+} Nano-crystals

Co^{2+} Concentration (mol %)	PL Peak Positions		
	Peak I (nm)	Peak II (nm)	Peak III (nm)
1	413	451	496
5	402	448	496
10	401	445	497
15	401	449	496
20	401	447	501

Table 2: Photoluminescence Peak Position in the ZnS:Ni^{2+} Nano-crystals

Ni^{2+} Concentration (mol %)	PL Peak Positions		
	Peak I (nm)	Peak II (nm)	Peak III (nm)
1	412	449	497
5	405	447	496
10	402	443	495
15	407	452	497
20	416	473	514

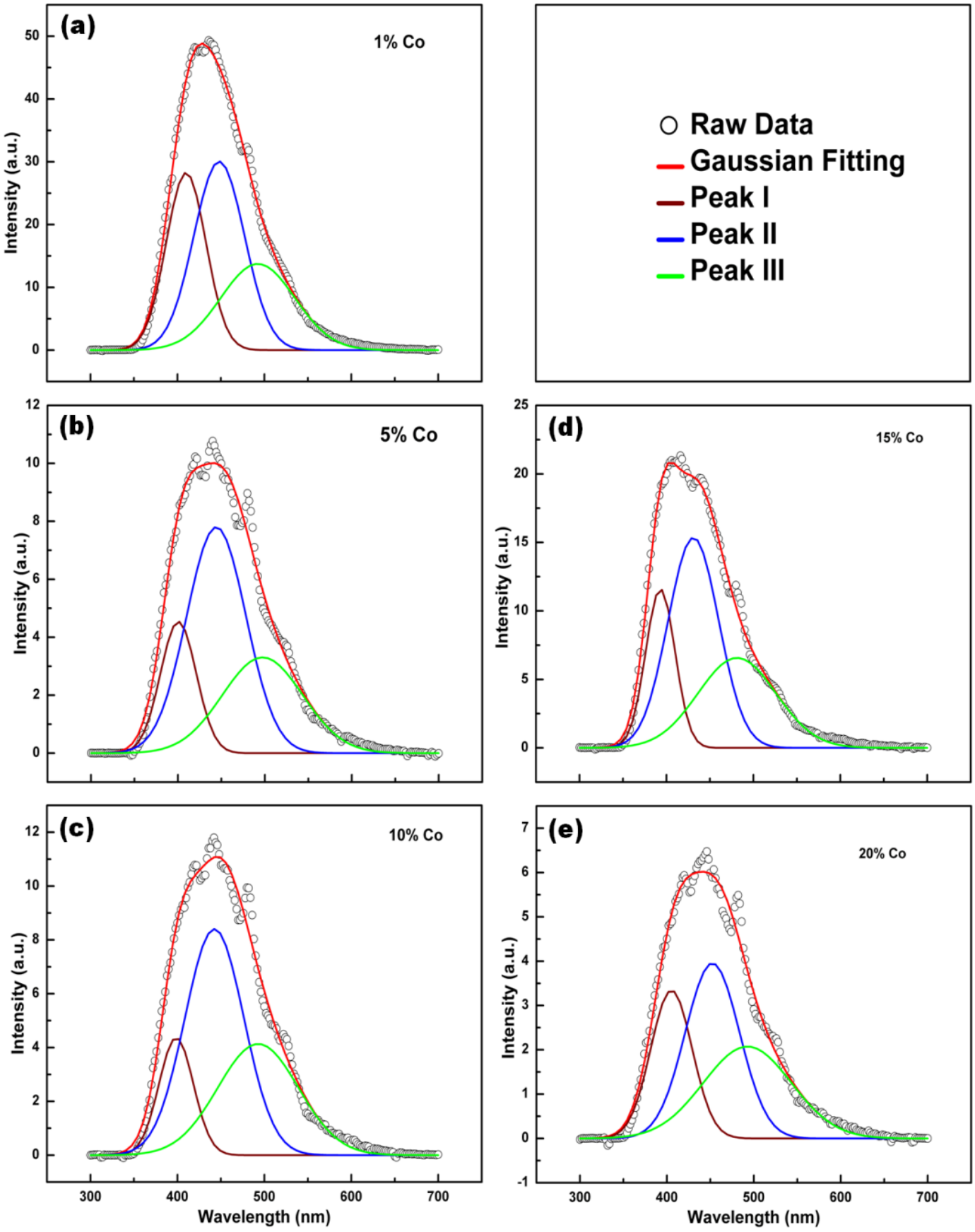

Fig. 4: Deconvoluted Photoluminescence Spectra of ZnS:Co^{2+} (a)1% (b)5% (c)10% (d)15% (e)20%.

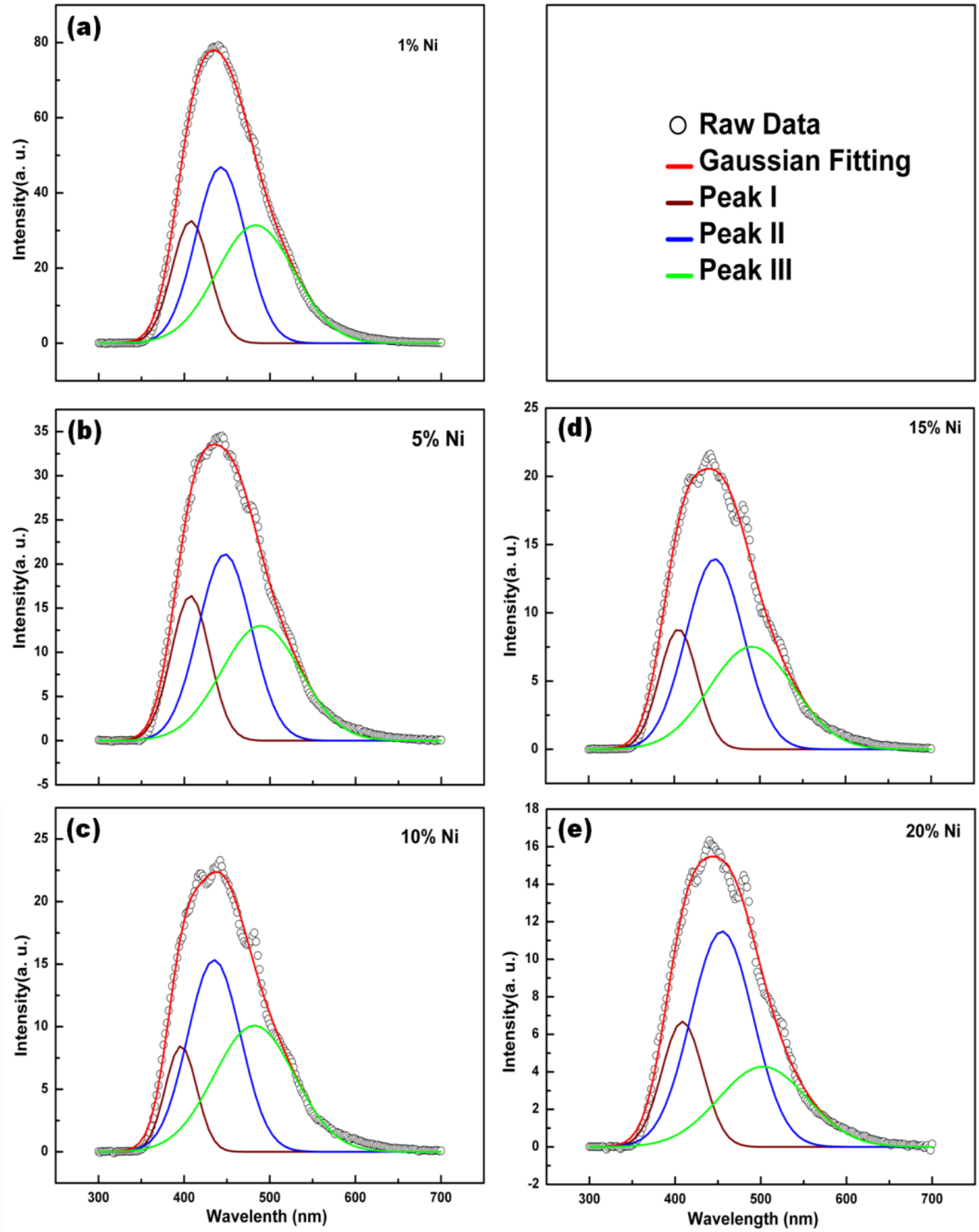

Fig. 5: Deconvoluted Photoluminescence Spectra of ZnS:Ni^{2+} (a)1% (b)5% (c)10% (d)15% (e)20%.

4. CONCLUSION

TM doped ZnS NCs were synthesized via wet chemical method using water/ethanol binary solution. The XRD and SEAD analysis show that the synthesized NCs were nearly spherical in shape, mono-dispersed and having narrow size distribution of 2-5 nm with no impurity phase at higher percentage of doping. Photoluminescence results showed that the PL intensity can be quenched by Cobalt and nickel doping. Due to quenching of PL intensity, the nickel and cobalt doped ZnS nano-crystals are unsuitable for the fluorescence-based application.

Conflict of Interest

The authors declare that they have no known competing financial interests or personal relationships that could have appeared to influence the work reported in this paper.

5. REFERENCES

1. Djazovski ON, Tanaka S, Kobayashi H, Semienov NN, Pasynkov VV. *Jpn. J. Appl. Phys.*, 1995; **34:**4819-4824.
2. Wang CW, Sheu TJ, Su YK, Yokoyama M. *Jpn. J. Appl. Phys.,* 1997; **36:**2728-2732.
3. Waldrip KE, Lewis JSIII, Zhai Q, Davidson MR, Holloway PH, Sun SS. *Appl. Phys. Lett.,* 2000; **76:**1276-1278.
4. Parsapour F, Kelley DF, Craft S, Wilcoxon JP. *J. Chem. Phys.,* 1996; **104:**4978-4987.
5. Monroy E, Omnes F, Calle F. *Semicond. Sci. Technol.,* 2003; **18:**R33-R51.
6. Chen R, Lockwood DJ. *J. Electrochem. Soc.,* 2002; **149:**s69-s78.
7. Nanda J, Sapra S, Sarma DD, Chandrasekharan N, Hodes G. *Chem. Mater.,* 2000; **12:**1018-1024.
8. Yu WW, Peng X. *Angew. Chem., Int. Ed.,* 2002; **41:**2368-2371.
9. Pradhan N, Katz B, Efrima S. *J. Phys. Chem.,* 2003; **107:**13843-13854.
10. Yu SH, Yoshimura M. *AdV. Mater.,* 2002; **14:**296-300.
11. Joo J, Na HB, Yu T, Yu JH, Kim YW, Mu F, et al. *J. Am. Chem. Soc.,* 2003; **125:**11100-11105.
12. Ma C, Li DM, Wang ZL. *AdV. Mater.,* 2003; **15:**228-231.
13. Jiang Y, Meng XM, Liu J, Hong ZR, Lee CS, Lee ST. *AdV. Mater.,* 2003; **15:**1195-1158.
14. Zhu YC, Bando Y, Xue DF, Golberg D. *J. Am. Chem. Soc.,* 2003; **125:**16196-16197.
15. Zhu YC, Bando Y, Xue DF. *Appl. Phys. Lett.,* 2003; **82:**1769-1771.
16. Brus L. *J. Phys. Chem.,* 1986; **90:**2555-2560.
17. Wang Y, Herron N. *J. Phys. Chem.,* 1991; **95:**525-532.
18. Alivisatos AP. *J. Phys. Chem.,* 1996; **100:**13226-13239.
19. Alivisatos AP. *Science,* 1996; **271:**933-937.
20. Chen CC, Herhold AB, Johnson CS, Alivisatos AP. *Science,* 1997; **276:**398-401.
21. Bhargava RN, Gallagher D, Hong X, Nurmikko D. *Phys. ReV. Lett.,* 1994; **72:**416-419.
22. Marking GA, Warren CS, Payne BJ. *U.S. Patent,* 2003; **6:**610 B2.
23. Lee S, Song D, Kim D, Lee J, Kim S, Park IY, et al. *Mater. Lett.,* 2004; **58:**342-346.
24. Alshawa AK, Lozykowski HJ. *J. Electrochem. Soc.,* 1994; **141:**1070-1074.
25. Jain M. II–IV Semiconductor Compounds. World Scientific Publishing Co. Pvt. Ltd.; 1994.
26. Xu SJ, Chua SJ, Liu B, Gan LM, Chew CH, Xu GQ. *Appl. Phys. Lett.,* 1998; **73:**478-480.
27. Bhargava RN, Gallagher D, Welker T, *J. Lumin.*,1994; **60-61:**275-280.
28. Chen W, Su F, Li G, Joly AG, Malm J, Bovin J, *J. Appl. Phys.* 2002; **92:**1950-1955.
29. Sun LD, Liu CH, Liao CS, Yan CH, *J. Mater. Chem.,* 1999; **9:**1655-1657.
30. Sun LD, Liu CH, Liao CS, Yan CH. *Solid State Commun.,* 1999; **111:**483-488.
31. Sun LD, Xu B, Fu XF, Wang MW, Qian C, Liao CH, et al. *Sci. China Ser. B.*, 2001; **44:**23-30.
32. Sooklal K, Cullum BS, Angel SM, Murphy CJ. *J. Phys. Chem.,* 1996; **100:**4551-4555.
33. Khosravi AA, Kundu M, Jatwa L, Deshpande SK. *Appl. Phys. Lett.,* 1995; **67:**2702-2704.
34. Murase N, Jagannathan R, Kanematsu Y, Watanabe M, Kurita A, Hirata K, et al. *J. Phys. Chem.,* 1999; **103:**754-760.
35. Bruchez M, Moronne M, Gin P, Weiss S, Alivisatos AP. *Science,* 1998; **281:**2013-2016.
36. Chan WCW, Nie SM. *Science,* 1998; **281:**2016-2018.
37. Peng ZA, Peng XG. *J. Am. Chem. Soc.,* 2001; **123:**183-184.
38. Peng X, Schlamp MC, Kadavanich AV, Alivisatos AP. *J. Am. Chem. Soc.,* 1997; **119:**7019-7029.
39. Kortan AR, Hull R, Opila RL, Bawendi MG, Steigerwald ML, Carroll PJ, et al. *J. Am. Chem. Soc.,* 1990; **112:**1327-1332.
40. Murphy CJ. *Anal. Chem.,* 2002; **74:**520A-526A.
41. Qu S, Yang H, Ren D, Kan S, Zou G, Li D, et al. *J. Colloid Interface Sci.,* 1999; **215:**190-192.
42. Domingo C, Rodriguez-Clemente R, Blesa M. *J. Colloid Interface Sci.,* 1994; **165:**244-252.
43. Jolivet P, Tronc E, Barbe C, Livage J. *J. Colloid Interface Sci.,* 1990; **138:**465-472.
44. Klong HP, Alexander LF. X-ray Diffraction Procedures, John Wiley and Sons:*New York*. 1954.
45. Cotton FA, Wilkinson G. Advanced Inorganic Chemistry, third ed., John Wiley & Sons, Inc., 1972.

46. Borse PH, Deshmukh N, Shinde RF, Date SK, Kulkarni SK. *J. Mater. Sci.,* 1999; **34:**6087-6093.
47. Karar N, Singh F, Mehta BR. *J. Appl. Phys.,* 2004; **95:**656-660.
48. Geng BY, Zhang LD, Wang GZ, Xie T, Zhang YG, Meng GW. *Appl. Phys. Lett.,* 2004; **84:**2157-2159.
49. Yang P, Lu M, Xu D, Yuan D, Song C, Liu S, et al . *Optical Materials,* 2003; **24:**497–502.
50. Jaffe PM, Banks E. *J. Electrochem. Soc.*, 1964; **111:**52-61.
51. Weakliem HA. *J. Chem. Phys.*, 1962; **36:**2117-2140.
52. Weller H, Koch U, Gutierrez M, Henglien A. *Ber. Bunsenges. Phys. Chem.*, 1984; **88:**649-656.